




Decoding volatile-microbial-physicochemical interplay of sensory preference in commercial shrimp paste based on flavoromics and high-throughput sequencing

Mengyue Hu^{a,b}, Ling Zhao^b, Huihui Sun^b, Qi Liu^b, Yong Xue^{a,**}, Rong Cao^{b,c,*} 

^a College of Food Science and Engineer, Ocean University of China, Qingdao, 266003, China

^b Yellow Sea Fisheries Research Institute, Chinese Academy of Fishery Sciences, Qingdao, 266071, China

^c Laboratory for Marine Drugs and Bioproducts, Qingdao Marine Science and Technology Center, Qingdao, 266237, China

ARTICLE INFO

Handling Editor: Professor Aiqian Ye

Keywords:

Commercial shrimp paste
Consumer preference
Key aroma compounds
Core functional microbiota
Formation pathways

ABSTRACT

Despite the long-standing tradition of shrimp paste in China, the aroma profiles driving consumer preferences remain poorly characterized. This study applied flavoromics and high-throughput sequencing to analyze nine commercial shrimp pastes, aiming to identify critical odorants influencing sensory acceptance and investigate their correlation with physicochemical properties and microbial communities. Nine distinct aroma attributes were identified as significant determinants of consumer preferences. Comprehensive volatile profiling using GC-IMS and GC-MS detected 44 and 40 volatiles, respectively, with 30 identified as aroma-active compounds (odor-active value ≥ 1). According to partial least squares regression analysis, fourteen key AACs significantly contributed to aroma attributes. Desirable AACs including 2,3-butanedione, isoamyl acetate, benzaldehyde, 2-heptanone, dimethyl trisulfide, 2,6-dimethyl pyrazine, 2,5-dimethyl pyrazine, and trimethyl pyrazine were associated with aroma attributes, such as sweet, meaty, cooked-garlic-like, sesame oil-like, and soy sauce-like aromas. Conversely, six AACs, including 3-methyl butanoic acid, naphthalene, trimethylamine, indole, 1-penten-3-ol, and Z-3-hexen-1-ol, contributed to off-odors characterized as pungent, earthy, rotten, and fishy. Significant variations were observed in physicochemical parameters and microbial composition, with dominant genera including *Tetragenococcus*, *Corynebacterium_1*, *Vagococcus*, *Acinetobacter*, *Alkalibacterium*, and *Psychrobacter* showing strong correlations with aroma formation. Metabolic pathway analysis revealed that microbial enzymatic activities-particularly decarboxylation, deamination, lysis, and lipid oxidation-critically shape the volatile profile through the degradation of amino acids and polyunsaturated fatty acids. This work systematically deciphers the molecular basis of shrimp paste flavor, providing actionable insights for optimizing fermentation processes to enhance sensory quality and consumer acceptance.

1. Introduction

Shrimp paste is a fermented seafood condiment, characterized by its distinctive flavor and umami taste. It is rich in protein, unsaturated fatty acids, bioactive peptides, astaxanthin, and other functional compounds beneficial to human health (Kleekayai et al., 2015). Additionally, shrimp paste can be stored stably for extended periods, thereby prolonging its shelf life. The history of shrimp paste consumption in China dates back more than 1500 years (Hu et al., 2024). Currently, China is a major producer, with an annual production of approximately 40,000 tons (Lu et al., 2022). The extensive coastline and diverse shrimp species in China

have resulted in a wide variety of shrimp paste products available on the market. Notable varieties include Bi jia shan shrimp paste (Jinzhou, Liaoning), Beitang shrimp paste (Tianjin), grasshopper sub shrimp paste (Rongcheng, Shandong), Ganyu shrimp paste (Lianyungang, Jiangsu), and Guangzhou smooth shrimp paste, each enjoying its market share in China.

The aroma of shrimp paste, determined by a variety of volatile compounds, plays a crucial role in consumer acceptance. Due to variations in environmental and processing conditions across different regions and factories, each brand of shrimp paste exhibits unique aroma profiles. To unravel the mysteries of shrimp paste flavor, researchers

* Corresponding author. Yellow Sea Fisheries Research Institute, Chinese Academy of Fishery Sciences, Qingdao, Shandong Province, 266071, China.

** Corresponding author. Ocean University of China, Qingdao, Shandong Province, 266003, China.

E-mail addresses: xueyong@ouc.edu.cn (Y. Xue), caorong@ysfri.ac.cn (R. Cao).

<https://doi.org/10.1016/j.crfs.2025.101050>

Received 20 February 2025; Received in revised form 17 March 2025; Accepted 9 April 2025

Available online 10 April 2025

2665-9271/© 2025 The Authors. Published by Elsevier B.V. This is an open access article under the CC BY-NC-ND license (<http://creativecommons.org/licenses/by-nc-nd/4.0/>).

have concentrated on understanding flavor changes during fermentation (Lv et al., 2020; Li et al., 2023a), the volatile differences among shrimp paste from diverse regions (Lu et al., 2022), and the effects of different fermentation conditions on volatile compounds (Yu et al., 2022a; Gao et al., 2024; Huang et al., 2024). Despite the long-standing tradition of shrimp paste consumption and numerous studies on the subject, there remains a lack of clarity regarding the aroma profiles preferred by contemporary Chinese consumers. Furthermore, these volatile compounds are generated through intricate metabolic pathways. Identifying the key pathways that influence the formation of essential odor compounds is vital for effective flavor regulation in shrimp paste.

The quality and flavor formation of fermented food are primarily attributed to the complex metabolic activities of microorganisms. During fermentation, these microorganisms secrete enzymes that hydrolyze fats and proteins into fatty acids, small peptides, and free amino acids, which serve as precursors for flavor development (Wang et al., 2025). In the context of shrimp paste fermentation, key microorganisms include *Tetragenococcus*, *Staphylococcus*, *Lactobacillus*, and *Bacillus* (Hu et al., 2024). Differences in raw materials and process conditions can significantly influence the function and composition of these microorganisms in shrimp paste. For example, *Lactobacillus* contributes notably to shrimp paste fermentation through its decarboxylase activity, which promotes the formation of pyrazine compounds (Che et al., 2021). Additionally, *Staphylococcus* has been observed to convert branched amino acids into branched volatile compounds, such as 2-methyl butanoic acid (Lv et al., 2020). Therefore, it is crucial to study the microbial composition and their correlation with volatile compounds to gain a comprehensive understanding of flavor formation in commercial shrimp paste.

Flavoromics systematically bridges sensory properties with aroma compounds through integrated sensory-instrumental-modeling frameworks, enabling precise decoding of flavor formation mechanisms (Hu et al., 2023). This approach synergizes gas chromatography-mass spectrometry (GC-MS) and headspace GC-ion mobility spectrometry (HS-GC-IMS) for comprehensive volatile profiling (Li et al., 2025). Multivariate techniques like partial least squares regression (PLSR) then establish quantitative aroma-sensory relationships by identifying key aroma-active compounds (AACs) (Wang et al., 2024). On the other hand, high-throughput sequencing (HTS) offers a comprehensive, accurate, and rapid approach to microbial analysis. HTS deciphers microbial functional dynamics in fermented products, and Pearson correlation analysis elucidates microbe-metabolite interactions (Wang et al., 2025). Together, this dual analytical axis – flavoromics mapping chemical-sensory linkages and HTS revealing microbial drivers – provides a multidimensional perspective for optimizing fermented food quality through targeted microbial and biochemical regulation.

In this study, we initially employed a flavoromics strategy to identify the active-aroma compounds (AACs) that influence consumer preference and the aroma profile of commercial shrimp paste. We further assessed microbial diversity and essential physicochemical indicators (moisture content, salinity, amino acid nitrogen (AAN), thiobarbituric acid reactive substances (TBARS), and total volatile base nitrogen (TVB-N)). We finally establish a correlation network between AACs, dominant microbiota, and physicochemical properties. Additionally, we preliminarily explored the potential formation pathways of AACs. By integrating these approaches, this research offers actionable insights for enhancing flavor profiles and improving quality control in shrimp paste production.

2. Materials and methods

2.1. Materials and chemicals

Nine commercial shrimp paste samples were purchased from five provinces across China: Liaoning, Tianjin, Shandong, Jiangsu, and Guangdong. These samples were primarily derived from three shrimp species (*Acetes chinensis*, *Neomysis awatschensis*, *Euphausia pacifica*) and

were spontaneously fermented in open clay jars under natural environmental conditions (10–35 °C ambient temperature) for 90–180 days, without exogenous starter cultures. Daily manual stirring (twice daily) ensured aerobic conditions. The origin, shrimp species, fermentation periods, and temperatures are provided in the Supplementary Material (Table S1). To preserve freshness, all were transported in ice boxes using cold-chain logistics and stored at –50 °C until further analysis.

For the instrumental analyses, n-ketone C4-C8 supplied by Sino-pharm Chemical Reagent Beijing Co., Ltd. (Beijing, China) were utilized in GC-IMS analysis to calculate retention index (RI) of each volatile compound. A n-alkane C6-C30 mixture (chromatographic grade, Supelco, Bellefonte, USA) was utilized in GC-MS analysis to calculate the linear retention indices of volatile compounds. 2, 4, 6-trimethylpyridine (≥99 % purity, Sinopharm Chemical Reagent Co., Ltd., Shanghai, China) was utilized as the internal standard in GC-MS analysis.

2.2. Sensory evaluation

Referring to Chen et al. (2022) and Lu et al. (2022) with some modifications. Five-gram samples of shrimp paste were incubated in 20 mL brown glass bottles at room temperature for 10 min before sensory evaluation. In the consumer preference test, sixty participants (30 men and 30 women, aged 15–55) from various regions of China, who temporarily reside in Qingdao, rated their preferences for the aroma of the nine shrimp paste samples on a scale from 1 (I dislike it very much) to 15 (I like it very much).

A descriptive sensory analysis was conducted by a panel of 20 students from the College of Food Science and Engineering, all of whom had completed a sensory discrimination test and were familiar with the sensory characteristics of shrimp paste. Panelists evaluated the intensity of nine identified aroma descriptors, as detailed in Table 1, on a scale from 0 (none) to 15 (very strong). All evaluations were performed in triplicate to ensure reliability.

2.3. HS-GC-IMS

Volatile compounds in the shrimp paste were identified using HS-GC-IMS (FlavourSpec, Dortmund, Germany) following a modified method previously utilized by our group (Hu et al., 2021). A 1.0-g sample of shrimp paste was placed in a 20 mL headspace vial and incubated in an agitator at 60 °C and 500 rpm for 10 min. Subsequently, 500 µL of the headspace gas was pre-separated using an MXT-WAX capillary column (15 m, 0.53 mm, 1.0 µdf) with nitrogen (N₂, 99.99 % purity) as the carrier gas. The carrier gas flow rate was programmed as follows: 2 mL/min for 2 min, 5 mL/min for 3 min, 15 mL/min for 5 min, 50 mL/min for 5 min, 100 mL/min for 5 min, and finally 150 mL/min for 5

Table 1

The detailed descriptions and references of nine aroma properties of shrimp paste.

Aroma terms	descriptions	Reference
Soy-sauce like	Salt, fermented, such as soy sauce.	2 g light soy sauce with 2 mL water put in a 20 mL headspace bottle
Sweet	Sweet, creamy	1 g Anchor Cheddar processed butter
Sesame oil-like	Cooked nutty, frying-peanut-oil odor	0.5 g sesame oil put in a 20 mL headspace bottle
Cooked garlic-like	Fermented cabbages, leek sauce	2 g roasted garlic
Meaty	Characteristic aroma of cook meat	2 g boiling shrimp pork meat
Fishy	Characteristic aroma of fish	0.5 g saury meat
Pungent	Burnt, intense odor, pungent	Over-burnt nuts
Earthy-like	Musty, characteristic odor of earth	5 g moist soil
Rotten	Stinky, rotten odor	5 g rotten shrimp meat

min. The analytes were ionized and further separated in the IMS ionization chamber. For identification purposes, n-ketones C4-C8 (Sino-pharm Chemical Reagent Beijing Co., Ltd, China) were used as external references to calculate the retention index (RI) of each volatile compound. The RI and drift time (DT) were then compared with the GC × IMS Library. The relative content of volatile compounds was quantified based on peak intensities.

2.4. SPME-GC-MS

A 20 mL headspace vial containing 5.0 g shrimp paste and 10 µL 2,4,6-trimethyl pyridine (internal standard, IS, at 5 ppm) was incubated at 60 °C for 15 min. Following this, an SPME fiber (DVB/CAR/PDMS, Supelco, USA) was introduced into the headspace vial to absorb volatile compounds at 60 °C for 30 min. The absorbed compounds were then desorbed in a GC injector at 250 °C for 5 min for analysis.

The separation and identification of volatile compounds were further accomplished using a GC-MS system (8890/7000D, Agilent Technologies Inc., USA) equipped with an INNOWAX chromatographic column (Agilent Technologies Inc., USA), following modified methods described by Lu et al. (2022). The desorbed substances were introduced into the GC-MS system using Helium (purity >99.999 %) in splitless mode. The column temperature was programmed as follows: initially set at 50 °C and held for 2 min, then increased to 150 °C at a rate of 5 °C/min and held for 2 min, and finally increased to 250 °C at a rate of 10 °C/min, maintaining this temperature for 5 min. MS was performed in full scan mode (m/z 29–350) with an ion source temperature of 230 °C.

To calculate the linear retention indices of volatile compounds, n-alkanes (C6-C30) were utilized. The identification of volatile compounds was based on a comparison of GC retention indices (RI) and mass spectra (MS) with the NIST 14 and Wiley11 libraries. The content of volatile compounds was calculated using the following equation:

$$\text{content (ng/g)} = \frac{\text{Peak area of volatile compounds}}{\text{Peak area of IS}} \times \frac{50 \mu\text{g}(\text{IS})}{5 \text{ g}(\text{sample})} \times 1000$$

2.5. (R)OAVs calculation

The OAV is commonly used to determine the contribution of volatile compounds to the overall aroma and is calculated as follows:

$$\text{OAV}_i = \frac{C_i}{\text{OT}_i}$$

C_i : the content of the volatile compound detected in the sample;

OT_i : the odor threshold of this compound found in the literature.

GC-IMS provides the concentration of volatile compounds based on peak intensity. To evaluate the specific contribution of each compound identified by GC-IMS, the relative OAV (ROAV) was employed, as detailed in previous studies (Xiao et al., 2022). The compound with the highest ratio of peak intensity to odor threshold is considered the most potent odorant, and its ROAV is regarded as 100. The ROAVs of other compounds are calculated using the following equation:

$$\text{ROAV}_i = \frac{\text{PI}_i}{\text{OT}_i} \times \frac{\text{OT}_{\max}}{\text{RI}_{\max}} \times 100$$

PI_i : the peak intensity of a volatile compound (i);

OT_i : the odor threshold of a volatile compound (i);

RI_{\max} : the peak intensity of the compound with the highest value calculated by dividing the relative content by the odor threshold;

OT_{\max} : the odor threshold of the compound with the highest value.

2.6. Measurement of physiochemical properties

Moisture was determined according to Chinese Standard GB5009.3–2016, using the direct drying method. Salinity was determined according to Chinese standard SC/T 3011-2001. AAN was

determined according to Chinese standard GB5009.235–2016, using the acidity meter method. TVB-N was determined according to Chinese standard GB5009.235–2016, adopting semi-trace nitrogen. TBARS measurement was determined according to Chinese standard GB 5009.181-2016.

2.7. Microbial diversity analysis

Bacterial DNA was extracted from shrimp paste samples using cetyltrimethylammonium bromide (CTAB). The 16S rDNA target region of the ribosomal RNA gene was amplified by PCR (90 °C for 5 min, followed by 30 cycles at 95 °C for 1 min, 60 °C for 1 min, and 72 °C for 1 min and a final extension at 72 °C for 7 min) using primers 341F (CCTACGGGGGCGWCAG) and 806R (GGACTACHVGGGTATCTAAT). Amplicons were evaluated with 2 % agarose gels, purified using the AMPure XP Beads (Beckman, CA, USA), and qualified by Qubit 3.0. Then, the sequencing libraries were generated using Illumina DNA Prep Kit (Illumina, CA, USA), were assessed with ABI StepOnePlus Real-Time PCR System (Life Technologies, Foster City, USA). At the end 2 × 250 bp paired-end reads were generated by sequencing on Novaseq 6000 platform. The raw reads were deposited into the NCBI Sequence Read Archive (SRA) database.

The raw sequencing data would be further filtered and analyzed using FASTP software (version 0.18.0) and QIIME software (v1.8.0). Operational taxonomic unit (OTU) clustering analysis was performed at sequence similarity of 97 % based on the UPARSE algorithm using USEARCH software (v10.0) and aligned by the BLAST algorithm.

2.8. Statistical analysis

Experiments were conducted in triplicate, and results are expressed as mean ± standard deviation. Statistical analysis was performed using SPSS 25 software (IBM, Armonk, USA). ANOVA with Duncan's test was utilized to determine significant differences, with $P < 0.05$ indicating statistical significance. Additionally, PLSR was performed using Unscrambler 9.7 software (CAMO ASA, Oslo, Norway) to investigate correlations between sensory attributes and active aroma compounds. Pearson correlation analysis was calculated in the R project psych package (version 1.8.4) through Omicsmart platform (<http://www.omicsmart.com>).

3. Results and discussion

3.1. Sensory evaluation analysis

Aroma preference plays a significant role in shaping consumer purchasing decisions (Simons et al., 2019). In our consumer preference test, panelists assigned the highest scores to sample SP8 (14.32 ± 0.26), and the lowest to SP4 (2.90 ± 0.13), as illustrated in Fig. 1A. This result highlights the substantial variability in flavor preference among commercial shrimp paste products. Based on the preference scores, the nine commercial shrimp paste samples were categorized into three distinct groups: the high-scoring group (HSP) comprising SP7, SP8, and SP9, with scores ranging from 13 to 15, the medium-scoring group (MSP) consisting of SP1, SP2, and SP3 with scores between 9 and 11, and the low-scoring group (LSP) including SP4, SP5, and SP6 with scores ranging from 3 to 5.

A descriptive sensory analysis identified nine key sensory attributes: “sesame oil-like”, “cooked garlic-like”, “soy sauce-like”, “meaty”, “rotten”, “fishy”, “earthy”, “pungent”, and “sweet”. Fig. 1B presents the intensity values of these attributes across shrimp paste samples, revealing significant differences in aroma profiles among the three groups. The MSP samples (SP1, SP2, and SP3) exhibited notably higher intensities of sesame oil-like, cooked garlic-like, soy sauce-like, and meaty attributes. The soy sauce-like odor, which has been reported in previous studies (Yu et al., 2022a,b; Fan et al., 2017; Lu et al., 2022), is

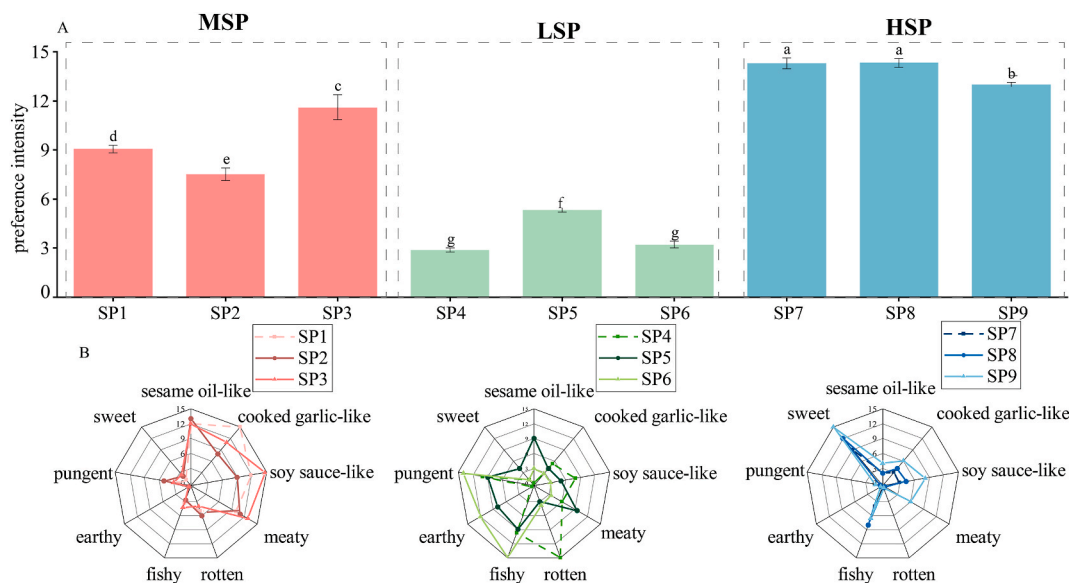


Figure 1. Scores of aroma preference (A) and aroma attributes (B) in nine commercial shrimp paste samples (MSP: shrimp pastes with medium preference scores; LSP: shrimp paste with low preference scores; HSP: shrimp paste with high preference scores.).

likely attributable to prolonged fermentation times or elevated salt content. Similarly, the cooked garlic-like attribute, characterized by a sulfur-like odor, is commonly associated with protein-rich fermented foods such as cheddar cheese and soybean paste (Chung and Chung, 2007; He and Chung, 2019). Despite these favorable attributes, MSP samples also exhibited subtle hints of undesirable odors, including fishy, rotten, and pungent odors. Interestingly, although the LSP group consistently received low preference scores, its samples exhibited distinct odor profiles. For instance, SP4 exhibited the highest intensity of the rotten odor (14.25 ± 0.30), while SP5 and SP6 were characterized by the strongest earthy odor. Additionally, all three LSP samples demonstrated elevated intensities of fishy odor. These undesirable attributes contributed to the low consumer preference scores in the LSP group, respectively. In contrast, the HSP group was distinguished by its dominant sweet odor, which emerged as the primary characteristic. The shrimp paste in this group also exhibited lower intensities of fishy, sesame oil-like, and cooked garlic-like odors, suggesting that the balance of these sensory attributes may have contributed to its higher consumer preference scores.

3.2. GC-IMS analysis

GC-IMS successfully isolated and identified fifty-four volatile compounds, including 11 alcohols, 8 aldehydes, 7 ketones, 11 esters, 3 sulfur-containing compounds (SCCs), 7 nitrogen-containing compounds (NCCs), 5 furans, and 2 additional compounds (Table S3). Significant differences in peak intensity were observed among the various types of shrimp paste (Fig. 2A). The MSP group (SP1, SP2, and SP3) exhibited the highest volatile intensity, with SCCs and ketones identified as the primary odorants. In contrast, the LSP group (SP4, SP5, and SP6) showed a marked decrease in total volatile intensities. Specifically, NCCs emerged as another abundant group in SP4, while alcohols and aldehydes accounted for a relatively high percentage in SP5 and SP6. Although alcohols and aldehydes also dominated the volatile profile in the HSP group, their concentrations were significantly lower than those in the LSP group.

To further elucidate the volatile profiles of different types of shrimp paste, a volatile heatmap was constructed (Fig. 2B). The MSP samples demonstrated higher concentrations of several key compounds, including dimethyl trisulfide, 2-heptanone, 2,5-dimethyl pyrazine, methyl pyrazine, trimethyl pyrazine, 2-octanone, 3-octanone, pentanoic

acid, propyl-butanoate, phenylacetaldehyde, 4-methyl-2-pentanol, hexyl acetate, and 2,3-pentanedione (Area I). Conversely, LSP samples were characterized by a greater abundance of compounds such as 2-acetyl furan, 2-hexanol, 2-phenylethanol, 3-methyl butanol, tetramethyl pyrazine, E-pentenal, 2-pentyl furan, 2-octanol, 3-methyl butanal, 2-ethyl furan, and Z-3-hexen-ol (Area II). Despite a significant reduction in volatile compounds in the HSP group, their flavor profile was primarily characterized by ethyl acetate, 2-furanmethanol, and pentyl acetate (Area III).

PCA was employed to elucidate the relationships among multiple variables by extracting a limited number of PCs. As shown in Fig. 2C, the total contribution ratio of the first two principal components reached 66 % (PC1 accounting for 46 % and PC2 for 20 %), exceeding the 60 % threshold and indicating sufficient characterization of similarities among different samples. The PCA score plot revealed that shrimp pastes with similar consumer preferences were closely clustered: MSP samples in red, LSP in green, and HSP in blue. Notably, shrimp pastes with different consumer preferences were distinctly distributed along the score value of PC1: MSP samples clustered in the positive region of PC1, LSP near zero, and HSP in the negative region. Thus, based on the result of GC-IMS analysis, shrimp paste with varying consumer preferences showed distinct volatile profiles.

3.3. GC-MS analysis

GC-MS identified 40 volatile compounds across the nine shrimp paste samples, including 6 alcohols, 5 aldehydes, 2 ketones, 5 acids, 5 SCCs, 10 NCCs, 3 alkanes, 2 furans, and 2 phenols, as detailed in Table S4. In comparison to GC-IMS, GC-MS detected fewer alcohols and aldehydes but identified a greater number of NCCs, SCCs, and acids, with phenols being exclusive to GC-MS. These discrepancies may stem from the differing analytical principles of each technique, suggesting that integrating GC-IMS and GC-MS could provide a more comprehensive volatile profile. As illustrated in Fig. 2D, NCCs constituted a significant portion of the volatile compounds across all shrimp paste samples. In addition to alkyl pyrazines detected by GC-IMS, compounds like indole and trimethylamine were prominent NCCs in high concentrations. The volatile content varied significantly among the three groups: MSP groups exhibited elevated levels of SCCs and phenols, while SCCs, alcohols, and aldehydes dominated LSP and HSP, respectively.

The heatmap of overall volatile compounds detected in GC-MS is

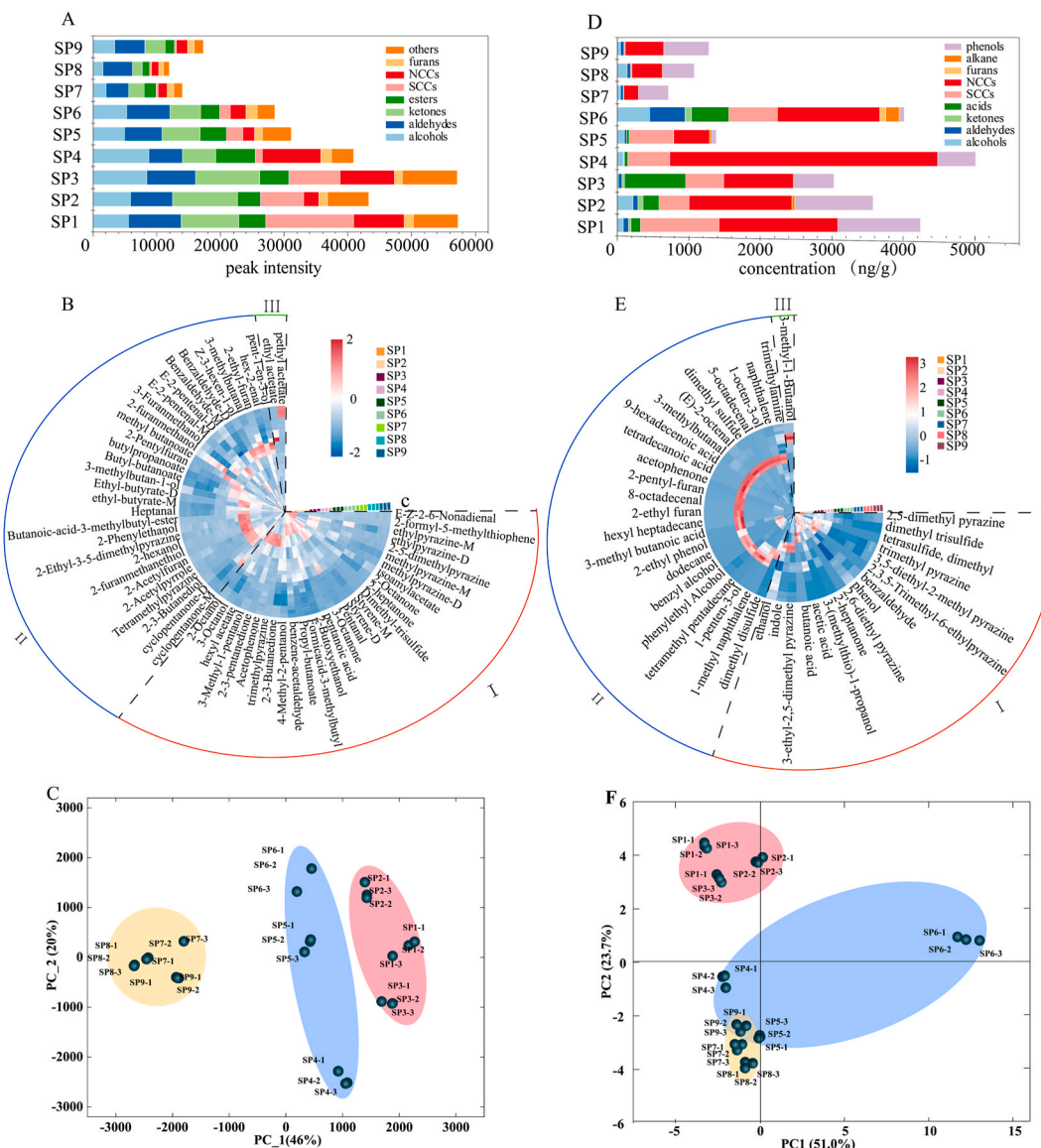


Figure 2. The profiles (A, D), heatmaps (B, E), and PCA scoring (C, F) of volatile compounds in commercial shrimp pastes detected by GC-IMS and GC-MS; (NCCs: nitrogen-containing compounds; SCCs: sulfur-containing compounds; M: monomer; M: monomer, D: dimer).

shown in Fig. 2E. MSP samples exhibited a diverse range of alkyl pyrazines with higher concentrations (Area I), including 2,3,5-trimethyl-6-ethyl pyrazine, 3,5-diethyl-2-methyl pyrazine, 3,5-dimethyl pyrazine, trimethyl pyrazine, and 2,5-dimethyl pyrazine, corroborating findings from GC-IMS. Notably, SP4 in the LSP group had elevated levels of indole, trimethylamine, and 3-ethyl-2,5-dimethyl pyrazine compared to other samples. SP5 and SP6 were characterized by higher concentrations of compounds such as naphthalene, 1-methyl naphthalene, 2-pentyl-furan, 8-octadecanal, 5-octadecenal, tetradecanoic acid, acetophenone, and 9-hexadecenoic acid. In contrast, HSP samples displayed significantly higher levels of 3-methyl butanol.

PCA based on the concentrations of these compounds (Fig. 2F) revealed that the first two principal components (PC1 and PC2) accounted for 51 % and 23.7 % of the total variation, respectively. This suggests that these components effectively capture the overall variation in the data. Cluster analysis indicated that MSP samples were distinctly positioned compared to LSP and HSP samples, which showed overlapping distributions. This finding suggests that GC-IMS is more effective than GC-MS at distinguishing the aroma profiles of shrimp paste, likely due to its capability to isolate more subtle volatile compounds,

such as aldehyde and alcohol.

3.4. OAV analysis

OAV analysis is a robust method for assessing the contribution of different volatile compounds to the overall aroma of food products. Compounds with higher OAVs indicate a greater impact on aroma perception. In this study, data obtained from GC-IMS and GC-MS were analyzed using ROAV and OAV methods, respectively, with the threshold of (R)OAV ≥ 1 used to identify AAC in shrimp paste. From the 55 volatiles identified by GC-IMS, 13 were classified as AACs, while 22 out of the 40 volatiles detected by GC-MS were identified as AACs. This resulted in a total of 30 AACs (Table 2), distributed as follows: 17 in SP1, 20 in SP2, 17 in SP3, 20 in SP4, 20 in SP5, 24 in SP6, 16 in SP7, and 13 in SP8 and SP9. Notably, the MSP group exhibited OVA summations ranging from 8500 to 19000, while OAVs for LSP ranged from 6000 to 15000, and those for HSP were below 1000.

Five specific SCCs were identified as AACs in shrimp paste: dimethyl trisulfide, dimethyl disulfide, dimethyl sulfide, 2-furanmethanethiol, and 3-methylthio-1-propanol. Due to their high concentrations and low

Table 2
Thresholds, odor descriptions, and (R)OAV of odorants for commercial shrimp paste.

AAC	Odor description	Threshold (mg/kg)	MSP			LSP			HSP		
			SP1	SP2	SP3	SP4	SP5	SP6	SP7	SP8	SP9
			ROAV								
dimethyl-trisulfide	onion, cabbage	0.05	100	100	100	16.69	100	100	17.53	18.34	12.24
2-3-butanedione	butter	0.1	18.08	24.40	28.75	69.69	93.20	85.58	100	100	100
2-furanmethanethiol	roasted	0.002	13.43	33.13	27.52	100	57.38	63.65	87.34	83.43	44.79
2-heptanone	meaty	1	1.64	4.01	2.16	0.71	1.53	1.10	1.73	1.10	0.73
3-methylbutanal	malty	1	1.05	2.98	0.83	1.31	3.19	15.38	12.73	9.44	3.26
styrene-M	sweet, floral	0.5	0.81	1.17	1.45	1.95	2.60	2.39	2.05	1.29	1.43
isoamyl acetate	fruity, banana	3.6	0.60	0.57	0.36	1.41	0.67	1.23	3.49	2.05	2.22
Z-3-hexen-1-ol	green	0.15	0.29	0.37	0.26	1.19	2.40	5.36	1.80	1.29	1.49
propyl-butanoate	sharp, rancid	0.2	0.27	0.59	0.38	0.54	0.71	1.58	1.02	0.45	0.34
pent-1-en-3-ol	green	0.8	0.16	0.32	0.23	0.77	0.82	3.19	2.25	1.12	0.88
2-acetylpyrrole	cooked potato	0.8	0.14	0.07	0.27	1.33	0.20	0.26	0.46	0.56	0.42
methyl butyrate	fruity, apple	1	0.06	0.15	0.11	0.20	1.05	1.93	1.04	0.57	0.36
2-ethyl-furan	n.f.	2.3	0.02	0.05	0.02	0.06	0.12	0.94	1.13	0.32	0.14
OAV											
benzaldehyde	almond-like	24	2.29	1.84	2.04	0.04	0.37	0.40	0.68	0.32	0.69
(E)-2-octenal	fatty, green	3	4.72	6.80	0.00	3.66	4.75	82.06	3.5	7.33	8.50
phenylethyl Alcohol	rose-like	9	9.62	16.89	2.28	2.93	0.95	22.78	0.86	–	1.03
trimethyl pyrazine	nut, coffee	4	16.93	13.25	19.41	12.26	1.20	2.23	2.44	1.1	5.26
2,6-diethyl pyrazine	nut, coffee	6	17.53	15.33	4.86	–	–	–	–	–	–
2-heptanone	meaty	1	43.99	48.78	31.84	4.64	–	10.21	–	–	0.00
phenol	phenolic	26	44.31	41.04	21.65	20.39	2.56	2.11	16.34	17.28	24.08
indole	feces-like	11	46.75	46.19	2.41	141.7	17.46	15.96	–	–	13.2
trimethylamine	fishy	2.4	68.98	41.70	83.88	130.2	87.60	306.4	56.17	161.4	102.4
3-(methylthio)-1-propanol	onion, meat-like	0.2	165.6	147.1	42.93	97.89	51.98	–	–	–	–
3,5-diethyl-2-methyl-pyrazine	nut, coffee	0.05	440.2	531.4	695.8	390.2	–	–	95.6	–	147.6
3-ethyl-2,5-dimethyl-pyrazine	nut, woody	1	566.5	571.9	394.8	1766	11.66	373.5	33.5	7.06	104.1
disulfide dimethyl	onion, cabbage	0.16	1659	414.8	596.1	1662	2945	61.25	22.94	42.88	42.88
dimethyl trisulfide	onion, cabbage	0.05	15580	6443	8196	5346	2255	933	204.2	222	229
1-penten-3-ol	green	0.8	–	63.37	–	–	113.3	257.2	–	–	–
dimethyl sulfide	onion, cabbage	0.05	–	–	–	–	609.4	12376	189	459.8	–
naphthalene	tar	6	–	–	–	–	2.83	14.73	1.31	0.94	–
1-methyl-naphthalene	tar	20	–	–	–	–	2.98	2.43	–	–	–
2-ethyl furan	n.f.	2.3	–	1.31	–	–	–	25.30	–	–	–
3-methyl butanal	malty	1	–	–	–	–	6.25	164.8	6.5	16.9	–
3-methyl butanoic acid	sweaty	46	–	0.67	0.48	–	0.39	3.76	–	–	–
2,5-dimethyl pyrazine	nut, coffee	0.80	152.9	40.53	70.31	51.77	8.81	–	10.64	19.23	29.93

Notes: n.f.: not found; -: not detected.

odor thresholds, these SCCs comprised over 60 % of the total OAV summation in most samples, underscoring their significant role in shaping the aroma of shrimp paste. Specifically, dimethyl trisulfide and 3-methylthio-1-propanol, commonly found in cooked or fermented foods, are associated with a meaty aroma (Liu et al., 2019; Zhang et al., 2020; Yao et al., 2024). Additionally, dimethyl trisulfide is known to enhance the umami aftertaste and palatability of dishes like soy miso (Inoue et al., 2016). These compounds showed remarkably higher OAVs in MSP compared to LSP and HSP. Conversely, dimethyl disulfide and dimethyl sulfide were more influential in the aroma profiles of LSP and HSP samples, with descriptors likening their odor to “intensely putrid” scents (Zang et al., 2017).

NCCs, comprising 10 components, were the most abundant AACs in shrimp paste. Among these, alkyl pyrazines — known for their cocoa, roasted nut, and potato-like aromas — are particularly influential in the overall aroma profile. Previous studies have identified trimethyl pyrazine, 3-ethyl-2,5-dimethyl pyrazine, and 2,5-dimethyl pyrazine as key odorants in traditional high-salt shrimp paste (Li et al., 2023b). Additionally, compounds like 2,6-diethyl pyrazine and 3,5-diethyl-2-methyl-pyrazine also contribute significantly to the characteristic aroma. Notably, 3-ethyl-2,5-dimethyl pyrazine exhibited the highest OAV in SP4, while the OAVs of other alkyl pyrazines were markedly higher in MSP samples. Trimethylamine, associated with a fishy odor in seafood, was more pronounced in the aroma of the LSP group. Indole and 2-acetyl pyrrole were notably higher in SP4, while 1-methyl-naphthalene and naphthalene were characteristic AACs of SP5 and SP6.

Alcohols (Z-3-hexen-1-ol, 1-penten-3-ol, phenylethyl alcohol), aldehydes (3-methyl butanal, benzaldehyde, E–2-Octenal), and ketones (2-heptanone, 2,3-butanedione) typically possess lower odor thresholds and significantly contribute to the flavor of shrimp paste. 1-Penten-3-ol, which generally imparts a fish-like odor, recorded the highest OAV of 275 in SP6. Similarly, 3-methyl butanal showed a high OAV of 165 in SP6, noted for its nutty, cheesy, and salty characteristics that contribute to a meaty aroma (Yang et al., 2024). However, excessive 3-methyl butanal can lead to undesirable flavors in meat products (Liu et al., 2019). Ketones also play a vital role in meat aroma due to their unique scents, ranging from fruity to creamy. In the HSP group, 2,3-butanedione emerged as the most potent AAC, while 2-heptanone had a higher OAV in MSP samples.

Other AACs, including isoamyl acetate, propyl butanoate, methyl butyrate, styrene, phenol, 2-methyl butanoic acid, and 2-ethyl furan, though exhibiting low OAVs, contribute less to the overall aroma profile of shrimp paste.

3.5. Correlation analysis between AACs and sensory attributes

To further elucidate the relationship between volatile compounds and the sensory attributes of shrimp paste, PLSR models were constructed, as illustrated in Fig. 3. In this model, the OAVs of AACs served as independent variables (X), while nine sensory properties were designated as dependent variables (Y). The resulting PLSR analysis revealed two factors that explained 72 % of the variance in both X and Y,

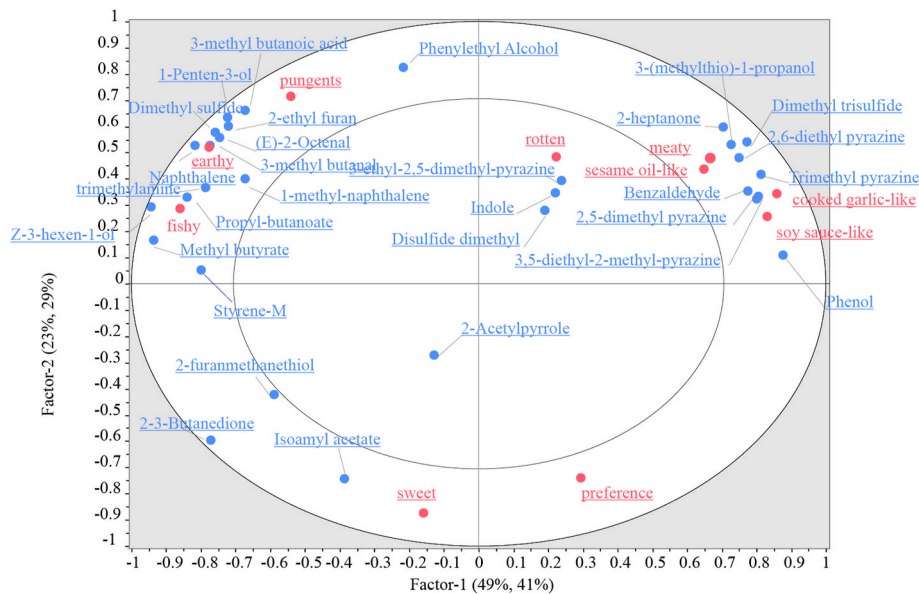


Figure_3. PLSR correlation loadings plot for volatile compounds with OAVs and aroma attributes in nine commercial shrimp paste samples.

indicating a robust model. The distribution of variances within the inner circle and outer ellipses (representing 50 % and 100 %, respectively) suggests that both sensory and volatile compound information can be effectively captured by PLSR (Zhao et al., 2024).

As shown in Fig. 3, sensory attributes are clustered into three distinct locations. Notably, the “sweet” odor and “preference” were located in the negative region of PC2, highlighting a positive correlation between these two attributes. The sweet aroma was strongly associated with volatile compounds like 2,3-butanedione and isoamyl acetate. Preference was also correlated positively with “sesame oil-like”, “meaty”,

“cooked garlic-like”, and “soy sauce-like” odors since all were positioned in the positive region of PC1. The “sesame oil-like” and meaty aroma correlated with benzaldehyde and 2-heptanone, while the “cooked garlic-like” scent was linked to dimethyl trisulfide. The “soy sauce-like” aroma showed strong correlations with 2,6-diethyl pyrazine, 2,5-dimethyl pyrazine, and trimethyl pyrazine. Conversely, pungent, earthy, and fishy odors were situated in the upper right quadrant, indicating a negative correlation with preference. The pungent aroma was primarily attributed to 3-methyl butanoic acid and 3-methyl butanal. The earthy scent was mainly linked to naphthalene, while the fishy

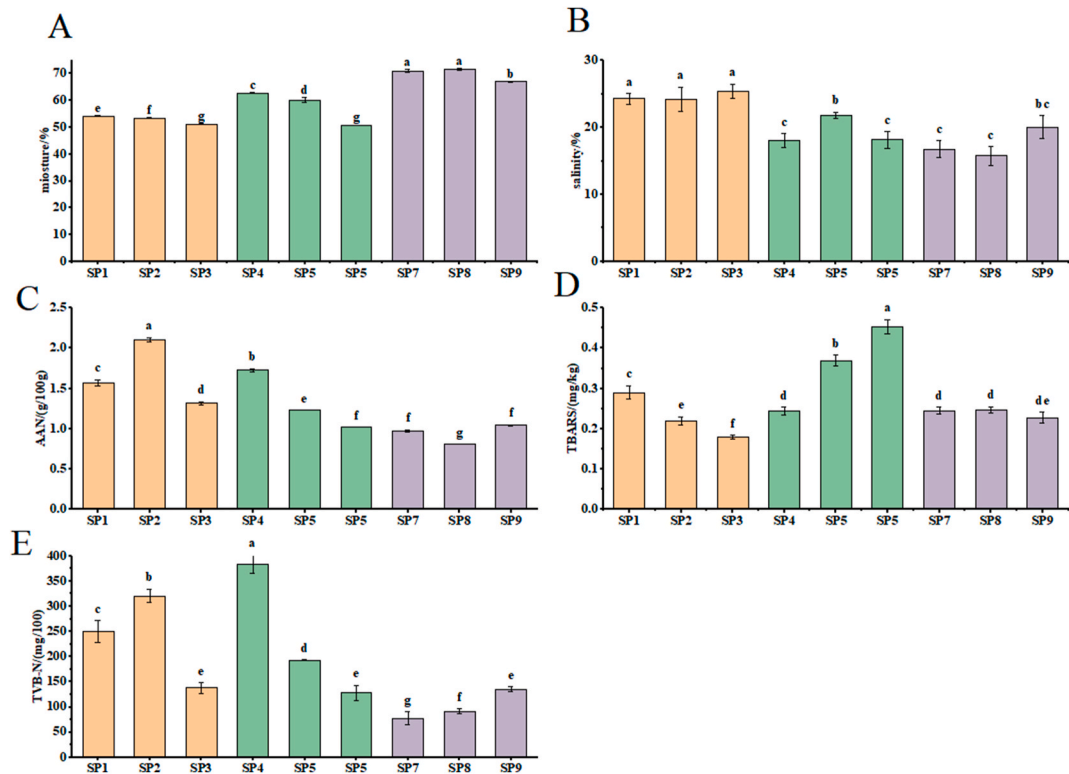


Figure 4. The moisture contents (A), salinity (B), AAN (C), TBARS (D), and TVB-N (E) of nine commercial shrimp pastes (ANN: amino acid nitrogen, TBARS: thiobarbituric acid reactive substances, TVB-N: total volatile base nitrogen.).

odor correlated with 1-penten-3-ol, trimethylamine, and Z-3-hexen-1-ol. Additionally, the rotten odor, characterized by a feces-like smell, was associated with indole. Overall, 14 of 30 AACs significantly contributed to shrimp paste aroma, including 2,3-butanedione, isoamyl acetate, benzaldehyde, 2-heptanone, dimethyl trisulfide, 2,6-diethyl pyrazine, 2,5-dimethyl pyrazine, trimethyl pyrazine, 3-methyl butanoic acid, 3-methyl butanal, naphthalene, 1-penten-3-ol, trimethylamine, and Z-3-hexen-1-ol, indole.

3.6. Physicochemical properties of commercial shrimp paste

The results of moisture, salinity, AAN, TVB-N, and TBARS analyses are shown in Fig. 4. The moisture content of nine commercial shrimp pastes ranged from 50.81 % to 71.72 %, with mean values of 52.97 % in the MSP group, 57.89 % in the LSP group, and 69.98 % in the HSP group. The HSP samples exhibited a higher moisture content compared to the other groups. Salinity levels varied between 15.76 and 25.42 g/100g with MSP samples showing the highest salinity. Notably, salinity influences the moisture content of shrimp paste as the lower salinity corresponds to higher water content (Jiang et al., 2024). Additionally, higher moisture content may result from the low fermentation temperature or shorter duration (Gao et al., 2024). The AAN content, a key indicator of the degree of proteolysis and a determinant of shrimp paste taste, ranged from 0.81 to 2.11 g/100g. The average AAN content was 1.67 g/100g in the MSP group, 1.33 g/100g in the LSP group, and 0.94 g/100g in the HSP group. TBARS, used to evaluate the degree of lipid oxidation (Wang et al., 2022), was below 0.3 mg/kg for all samples, except for SP5 (0.37 mg/kg) and SP6 (0.45 mg/kg) in the LSP group. The TVB-N values, which reflect product freshness and spoilage caused by bacteria metabolism and endogenous enzyme activity, ranged from 77.90 to 384.72 mg/100g in commercial shrimp paste samples (Yang et al., 2021). SP4 exhibited the highest TVB-N value (380 mg/100g). In summary, HSP samples, characterized by the highest moisture content and lower chemical values suggest mild fermentation, likely due to lower fermentation temperature or shorter duration. Conversely, the elevated AAN content in MSP indicates strong proteolysis during fermentation. The high TVB-N or TBARS in LSP samples point to intense chemical reactions in their processing.

3.7. Microbiological analysis

In the analysis of nine shrimp paste samples, a total of 2723 bacterial OTUs were identified. To explore the characteristics of OTUs among different samples, we conducted a Venn diagram analysis based on OTU abundance. The analysis revealed that only 115 OTUs were common

across nine shrimp paste samples, constituting merely 4 % of the total OTUs. The number of unique bacterial OTUs were found to be 376 in SP1, 362 in SP2, 254 in SP3, 354 in SP4, 428 in SP5, 209 in SP6, 222 in SP7, 57 in SP8, and 346 in SP9. These findings suggest that while commercial shrimp pastes share some common microbial communities, they also possess more distinct microbial communities. The relative abundances of the prevalent microbiota are depicted in Fig. 5. At the phylum level, 24 phyla were identified, with *Firmicutes* and *Proteobacteria* being the most dominant. At the genus level, *Tetragenococcus* was identified as the dominant genus in commercial shrimp paste, exhibiting a relative abundance of more than 1 % in all samples. Other major genera, including *Corynebacterium_1*, *Lactobacillus*, *Vibrio*, *Psychrobacter*, and *Vagococcus*, were also prevalent in commercial shrimp paste.

The abundance of bacterial taxa varied across different samples, and distinct biomarkers distinguishing the shrimp paste samples were identified using the Kruskal-Wallis H test. A total of 121 microbial community groups were found to be significantly different among the nine samples ($P < 0.05$). Fig. 6 highlights the top 10 dominant genera. Notably, *Tetragenococcus* showed markedly higher abundance in SP6 and SP8, while *Corynebacterium_1* and *Alkalibacterium* characterized SP3. *Vagococcus* and *Psychrobacter* were prevalent in SP7, and *Acinetobacter* exhibited higher abundance in SP1 and SP4. In summary, the microbial distribution among commercial shrimp pastes is characterized by significant variations, with specific microbial groups playing crucial roles in each sample. The marked differences in the relative abundance of *Tetragenococcus*, *Corynebacterium_1*, *Vagococcus*, *Acinetobacter*, *Alkalibacterium*, and *Psychrobacter* emphasize their significant contributions to the flavor variations in commercial shrimp paste.

3.8. Correlation analysis between AACs and microbial-physicochemical factors

To further understand the relationship between microbial communities and quality factors among commercial shrimp paste, we performed a Pearson correlation analysis between dominant bacterial genera and key AACs. Most of the genera were found to exhibit a certain degree of correlation with AACs. The results, illustrated in Fig. 7, reveal several noteworthy correlations. *Tetragenococcus* exhibited positive correlations with TBA (correlation coefficient (r) = 0.69) and a range of off-odorants (r = 0.43–0.72), including Z-3-hexen-ol (C5), propyl butanone (C6), methyl butyrate (C8), (E)-2-octenal (C10), phenylethyl alcohol (C11), trimethylamine (C17), 1-penten-3-ol (C23), dimethyl sulfide (C24), naphthalene (C25), 2-ethyl furan (C27), and 3-methyl butanoic acid (C29). This genus is recognized for its substantial production of lipases, which contribute to the accumulation of free fatty

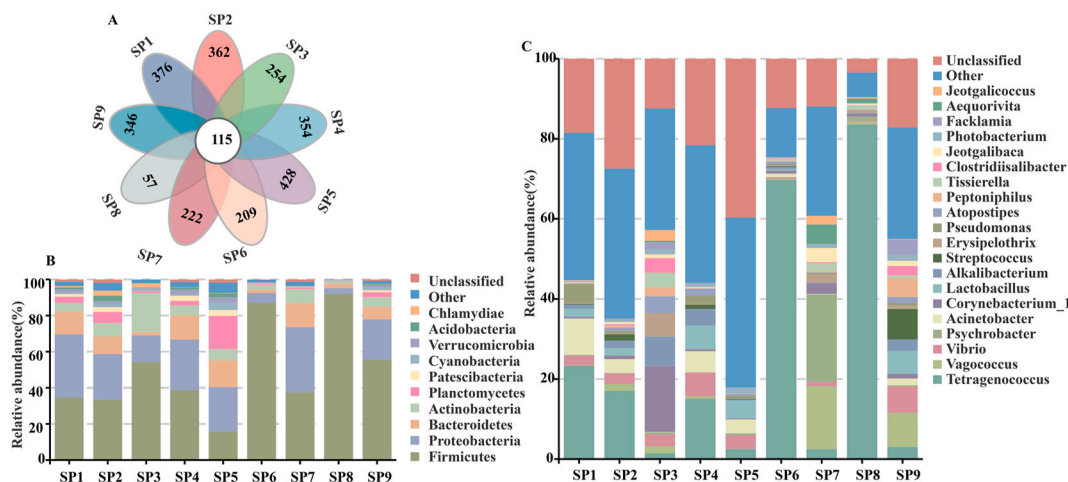


Figure 5. Microbial profiles of commercial shrimp pastes. (A) Venn plots of bacteria OUT. (B) The relative abundance of top 10 abundant communities at phylum level; (C) The relative abundance of top 20 abundant communities at genus level.

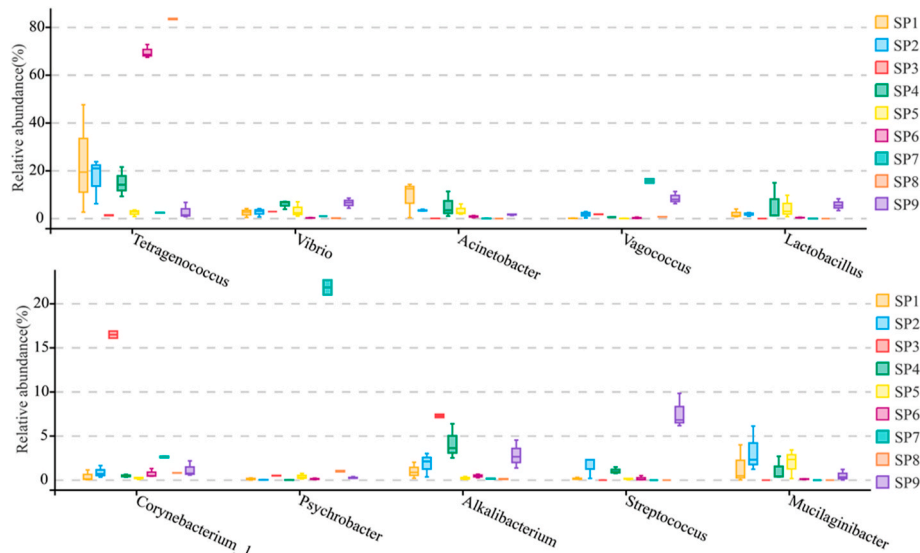


Figure 6. Analysis of microbial differences among commercial shrimp pastes by Kruskal-Wallis H test.

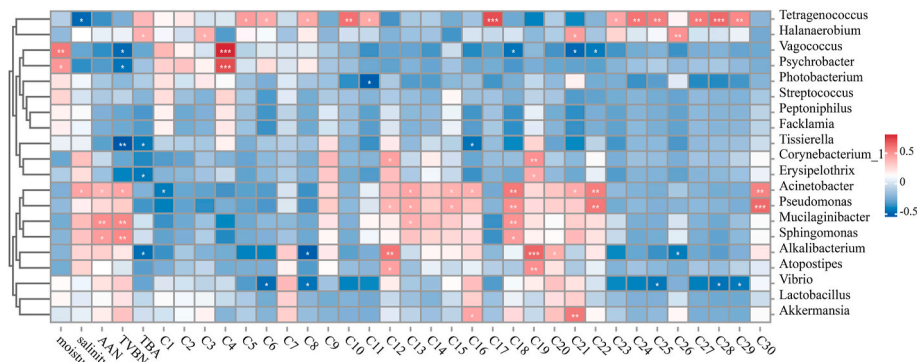


Fig. 7. Correlation analysis between dominant bacteria, physicochemical properties, and AACs in shrimp pastes. *, $P < 0.05$; **, $P < 0.01$; ***, $P < 0.001$ (ANN: amino acid nitrogen, TBARS: thiobarbituric acid reactive substances, TVB-N: total volatile base nitrogen, C1-C30: 30 aroma-active compounds).

acids and the formation of distinctive odorants in shrimp paste (Li et al., 2023a). Additionally, *Tetragenococcus* displayed a negative correlation with both salinity ($r = -0.46$, $p < 0.05$) and moisture content ($r = -0.35$), suggesting that elevated salinity or moisture levels may inhibit its growth. Conversely, *Acinetobacter* and *Pseudomonas* exhibited significant positive correlations with TVB-N, AAN, and various AACs, such as trimethyl pyrazine (C12), 2,6-diethyl pyrazine (C13), 3-methylthio-1-propanol (C18), dimethyl trisulfide (C22), and 2,5-dimethyl pyrazine (C30), highlighting their pivotal role in proteolysis. Their positive association with indole further underscores the potential risk of flavor deterioration in shrimp paste due to their over-accumulation. Previous studies have also indicated that *Acinetobacter* is positively correlated with the production of various biogenic amines, attributed to its high proteolytic activity (Hua et al., 2025). Therefore, managing the growth of *Acinetobacter* and *Pseudomonas* is essential to enhance both the flavor and safety of shrimp paste. Furthermore, 2,3-butanedione and isoamyl acetate were closely associated with bacterial genera such as *Psychrobacter* and *Vagococcus*, which demonstrated positive correlations with moisture. This suggests that mild fermentation conditions could favor the growth of *Psychrobacter* and *Vagococcus*, thereby contributing to improved shrimp paste flavor.

3.9. Analysis of potential sources of aroma-active compounds in shrimp paste

To understand the aroma formation mechanism in shrimp paste, potential precursors and metabolic processes of AACs were predicted according to physicochemical properties, literature, KEGG databases, and the MetaCyc platform. The aroma-active compounds in shrimp paste primarily arise from amino acid degradation, carbohydrate metabolism, lipid degradation and oxidation, microbial esterification, and other auxiliary processes (Fig. 8).

During fermentation, microorganisms break down proteins and peptides into free amino acids, facilitating the production of various volatile compounds. Among the 30 identified AACs, 19 odorants—including dimethyl trisulfide, 2-furanmethanethiol, 3-methyl butanal, phenol, etc.—originate from amino acid metabolism, highlighting its significant role in flavor formation. These compounds emerge from four metabolic processes: decarboxylation, deamination, lysis reaction, and Strecker degradation. For example, alkylpyrazines are formed through the condensation of aminoacetones, which originate from the decarboxylation of amino acids through threonine 3-dehydrogenase or glycine C-acetyltransferase (Zhang et al., 2019; Lv et al., 2020; Che et al., 2021). Branched-chain compounds such as benzaldehyde, phenylethyl alcohol, 3-methyl butanal, 3-methyl butanoic acid, and 3-(methylthio)-1-propanol are deamination products of phenylalanine, leucine, and methionine through dehydrogenase or transaminase (Beck

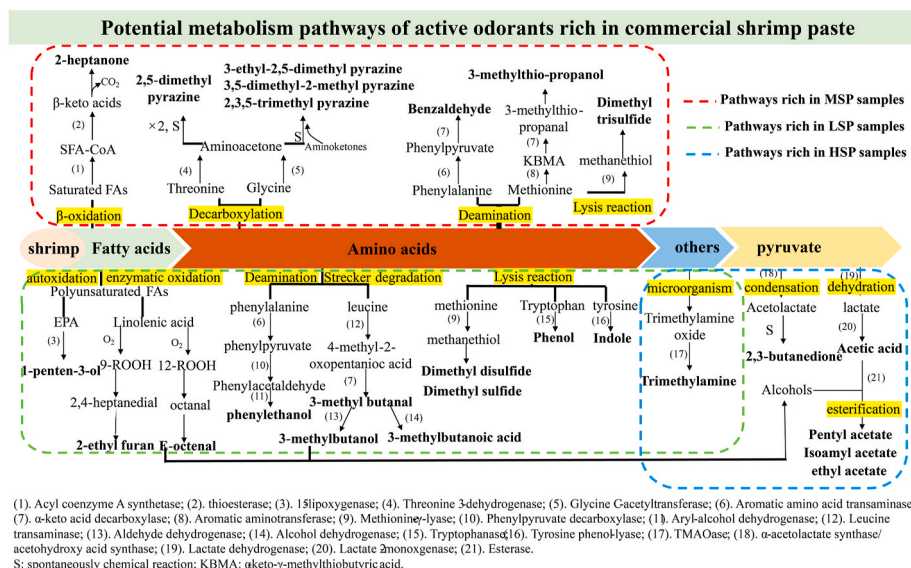


Fig. 8. Sketch map of potential sources of the aroma active compounds in commercial shrimp paste (MSP: shrimp pastes with medium preference scores; LSP: shrimp paste with low preference scores; HSP: shrimp paste with high preference scores.).

et al., 2002; Nierop Groot and de Bont Jan, 1999). Previous studies highlighted that high-salt shrimp paste typically contains elevated levels of volatile acids, aldehydes, and heterocyclic compounds which might explain why they exhibited higher contents in MSP samples (Yu et al., 2022b). Additionally, methionine, tyrosine, and tryptophan can degrade into methanethiol, indole, and phenol through amino acid lyases (Feng et al., 2021). Methanethiol subsequently oxidizes into various sulfur-containing compounds (Martínez-Cuesta et al., 2013). Based on TVB-N and the volatile contents, the over-degradation of amino acids results in the over-accumulation of indole, 3-methyl butanal, and dimethyl sulfide, deteriorating the shrimp paste flavor.

Aliphatic odorants, including 2-heptanone, Z-3-hexen-1-ol, and 1-penten-3-ol, stem from the oxidation of saturated or unsaturated fatty acids (FA). During fermentation, bacteria metabolize fatty acids via β -oxidation, generating acyl-coenzyme A (CoA) for energy. This process converts fatty acid acyl-CoA derivatives into shorter chain acyl CoA by losing two carbon atoms (Shahidi and Abad, 2019). Incomplete β -oxidation results in methyl ketones, particularly 2-methyl ketones (Li and Ma, 2014). Conversely, the chemical or enzymatic oxidation of polyunsaturated fatty acids (PUFAs) leads to the formation of various aldehydes, alcohols, and furans. PUFAs react with active oxygen to produce hydroperoxides, which transform to yield secondary compounds; for instance, 1-penten-3-ol is the oxidation product of eicosapentaenoic acid (Wu et al., 2021). Compared with HSP and MSP, the PUFA-derived odorants and TBARS in LSP increased significantly.

Carbohydrate metabolism is vital for flavor formation, primarily by generating pyruvate. Pyruvate can condense and decarboxylate to form 2,3-butanedione and acetate (Kleerebezemab et al., 2000). Acetate may esterify with alcohols from amino acid or lipid degradation. The higher levels of 2,3-butanedione, ethyl acetate, pentyl acetate, and isoamyl acetate in HSP samples indicate significant carbohydrate metabolism is good for shrimp paste flavor. Additionally, trimethylamine arises from the microbial reduction of trimethylamine oxide. Research shows that certain lactic acid bacteria from traditional fermented foods can utilize trimethylamine for growth (Park et al., 2020). Therefore, inoculating lactic acid bacteria during fermentation could help decrease trimethylamine levels to enhance flavor.

4. Conclusion

This study investigates the intricate interactions among sensory

characteristics, volatile composition, physicochemical parameters, and microbial communities in commercial shrimp paste. Sensory profiling identified nine key aroma attributes, comprising both desirable notes (e.g., sweet, soy sauce-like, sesame oil-like, cooked garlic-like, meaty) and off-odors (e.g., rotten, fishy, earthy, pungent). Through the combined application of GC-IMS and GC-MS, a high-resolution volatile fingerprint was constructed, identifying 30 aroma-active compounds (AACs) with odor activity values (OAVs) ≥ 1 . Partial least squares regression analysis highlighted that fourteen key AACs significantly contributed to aroma attributes. And Pearson correlation analysis revealed critical microbial and physicochemical factors influencing flavor development. Mild fermentation conditions that favor the growth of *Psychrobacter* and *Vagococcus* were associated with the production of beneficial AACs, such as 2,3-butanedione and isoamyl acetate, via metabolic pathways like pyruvate conversion and esterification. These conditions contributed to the development of a premium flavor profile. Similarly, high-salinity fermentation, which supported the presence of *Acinetobacter* and *Pseudomonas* facilitated the generation of desirable compounds, such as alkyl pyrazines and dimethyl trisulfide, through amino acid metabolism. In contrast, excessive proliferation of *Tetragenococcus*, *Acinetobacter*, and *Pseudomonas* in low-salt samples accelerated the catabolism of tyrosine, leucine, methionine, and PUFAs, leading to the formation of off-flavor compounds, including indole, 3-methyl butanoic acid, dimethyl sulfide, Z-3-hexenol, and 1-penten-3-ol. These findings underscore two distinct metabolic pathways governing flavor evolution: (1) enzymatic refinement under optimal fermentation conditions, such as high salinity, low temperature, or short fermentation duration, which generates aroma-enhancing volatiles, and (2) proteolytic and lipolytic overactivity under dysbiosis conditions, such as low-salinity fermentation, which produces sensory-deteriorating metabolites. The identified correlations between microbial taxa and volatile biomarkers provide actionable insights for optimizing fermentation protocols, enabling the suppression of off-odor formation while enhancing consumer-preferred aroma profiles. While correlations suggest microbial contributions to aroma formation, future metatranscriptomic studies are required to validate enzymatic pathways.

CRediT authorship contribution statement

Mengyue Hu: Writing – original draft, Visualization, Investigation.
Ling Zhao: Conceptualization, Writing – review & editing. **Huihui Sun:**

Writing – review & editing. **Qi Liu:** Conceptualization. **Yong Xue:** Supervision. **Rong Cao:** Project administration, Funding acquisition.

Ethical statement

The authors ensure that the work described has been carried out in accordance with The Code of Ethics of the World Medical Association (Declaration of Helsinki) for experiments involving humans. The authors confirm that appropriate protocols for protecting the rights and privacy of all participants were utilized during the execution of the research. Participants provided informed consent by affirmatively responding to the statement, “I am aware that my responses are confidential, and I agree to participate in this sensory evaluation,” which was a prerequisite for participation. Furthermore, participants were informed of their right to withdraw from the sensory evaluation at any time without providing a reason.

Declaration of competing interest

The authors declare that they have no known competing financial interests or personal relationships that could have appeared to influence the work reported in this paper.

Acknowledgments

This work was supported by Key R&D Program Project of Shandong Province [2023TZXD052]; Central Public-interest Scientific Institution Basal Research Fund, YSFRI, CAFS [NO. 20603022023017]; and Central Public-interest Scientific Institution Basal Research Fund, CAFS [NO.2023TD72].

Appendix A. Supplementary data

Supplementary data to this article can be found online at <https://doi.org/10.1016/j.crfs.2025.101050>.

Data availability

Data will be made available on request.

References

- Beck, H.C., Hansen, A.M., Lauritsen, F.R., 2002. Metabolite production and kinetics of branched-chain aldehyde oxidation in *Staphylococcus xylosus*. *Enzym. Microb. Technol.* 31 (1), 94–101. [https://doi.org/10.1016/S0141-0229\(02\)00067-4](https://doi.org/10.1016/S0141-0229(02)00067-4).
- Che, H., Yu, J., Sun, J., Lu, K., Xie, W., 2021. Bacterial composition changes and volatile compounds during the fermentation of shrimp paste: dynamic changes of microbial communities and flavor composition. *Food Biosci.* 43, 101169. <https://doi.org/10.1016/j.fbio.2021.101169>.
- Chen, C., Tian, T., Yu, H., Yuan, H., Wang, B., Xu, Z., Tian, H., 2022. Characterisation of the key volatile compounds of commercial Gouda cheeses and their contribution to aromas according to Chinese consumers' preferences. *Food Chem. X* 15, 100416. <https://doi.org/10.1016/j.fochx.2022.100416>.
- Chung, L., Chung, S.-J., 2007. Cross-cultural comparisons among the sensory characteristics of fermented soybean using Korean and Japanese descriptive analysis panels. *J. Food Sci.* 72 (9), S676–S688. <https://doi.org/10.1111/j.1750-3841.2007.00542.x>.
- Fan, Y., Yin, L., Xue, Y., Li, Z., Hou, H., Xue, C., 2017. Analyzing the flavor compounds in Chinese traditional fermented shrimp pastes by HS-SPME-GC/MS and electronic nose. *J. Ocean Univ. China* 16 (2), 311–318. <https://doi.org/10.1007/s11802-017-3194-y>.
- Feng, L., Tang, N., Liu, R., Gong, M., Wang, Z., Guo, Y., Wang, Y., Zhang, Y., Chang, M., 2021. The relationship between flavor formation, lipid metabolism, and microorganisms in fermented fish products. *Food Funct.* 12 (13), 5685–5702. <https://doi.org/10.1039/D1FO00692D>.
- Gao, R., Xue, J., Shi, T., Li, Y., Yuan, L., 2024. Effects of ‘bask in sunlight and dewed at night’ on the formation of fermented flavor in shrimp paste after maturation. *Food Chem.* 452, 139546. <https://doi.org/10.1016/j.foodchem.2024.139546>.
- He, W., Chung, H.Y., 2019. Comparison between quantitative descriptive analysis and flash profile in profiling the sensory properties of commercial red sufu (Chinese fermented soybean curd). *J. Sci. Food Agric.* 99 (6), 3024–3033. <https://doi.org/10.1002/jsfa.9516>.
- Hu, B., Zhang, C., Chu, B., Gu, P., Zhu, B., Qian, W., Chang, X., Yu, M., Zhang, Y., Wang, X., 2023. Unraveling the relationship between key aroma components and sensory properties of fragrant peanut oils based on flavoromics and machine learning. *Food Chem. X* 20, 100880. <https://doi.org/10.1016/j.fochx.2023.100880>.
- Hu, M., Wang, S., Liu, Q., Cao, R., Xue, Y., 2021. Flavor profile of dried shrimp at different processing stages. *LWT–Food Sci. Technol.* 146. <https://doi.org/10.1016/j.lwt.2021.111403>.
- Hu, M.-Y., Zhao, L., Sun, H.-H., Xue, Y., Mao, X.-Z., Cao, R., 2024. Recent advances on shrimp paste: key flavor components and biochemical formation pathways, biogenic amine formation, microbial functions, and innovative process strategies. *Trends Food Sci. Technol.* 152, 104694. <https://doi.org/10.1016/j.tifs.2024.104694>.
- Hua, X., Yan, T., Liu, S., Yin, L., Jia, X., 2025. Insights into the correlation between bacterial community succession and dynamics of biogenic amines during three types of sufu fermentation. *Food Control* 168, 110870. <https://doi.org/10.1016/j.foodcont.2024.110870>.
- Huang, J., Liu, Y., Shang, S., Zhu, K., Miao, X., Dong, X., Jiang, P., 2024. Changes in bacterial flora and flavor of shrimp paste under different salt concentrations. *LWT–Food Sci. Technol.* 205, 116534. <https://doi.org/10.1016/j.lwt.2024.116534>.
- Inoue, Y., Kato, S., Saikusa, M., Suzuki, C., Otsubo, Y., Tanaka, Y., Watanabe, H., Hayase, F., 2016. Analysis of the cooked aroma and odorants that contribute to umami aftertaste of soy miso (Japanese soybean paste). *Food Chem.* 213, 521–528. <https://doi.org/10.1016/j.foodchem.2016.06.106>.
- Jiang, P., Liu, Y., Yang, J., Cai, W., Jiang, C., Hang, J., Miao, X., Sun, N., 2024. Feasibility of circular fermentation as a new strategy to accelerate fermentation and enhance flavor of Antarctic krill paste. *Curr. Res. Food Sci.* 9, 100838. <https://doi.org/10.1016/j.crfs.2024.100838>.
- Kleekayai, T., Harnedy, P.A., O’Keeffe, M.B., Poyarkov, A.A., CunhaNeves, A., Suntornusuk, W., FitzGerald, R.J., 2015. Extraction of antioxidant and ACE inhibitory peptides from Thai traditional fermented shrimp pastes. *Food Chem.* 176, 441–447. <https://doi.org/10.1016/j.foodchem.2014.12.026>.
- Kleerebezemab, M., Hols, P., Hugenholtz, J., 2000. Lactic acid bacteria as a cell factory: rerouting of carbon metabolism in *Lactococcus lactis* by metabolic engineering. *Enzym. Microb. Technol.* 26 (9), 840–848. [https://doi.org/10.1016/S0141-0229\(00\)00180-0](https://doi.org/10.1016/S0141-0229(00)00180-0).
- Li, L., Ma, Y., 2014. Effects of metal ions on growth, β -oxidation system, and thioesterase activity of *Lactococcus lactis*. *J. Dairy Sci.* 97 (10), 5975–5982. <https://doi.org/10.3168/jds.2014-8047>.
- Li, J., Zhou, H., Xu, L., Yu, C., Hu, M., Zhong, B., Tu, Z., Peng, B., 2025. Exploration of the changes in volatile flavor compounds of low salt dry-curing grass carp (*Ctenopharyngodon idella*) blocks during cold storage detected by E-nose, HS-SAFE-GC-MS and HS-GC-IMS. *LWT - Food Sci. Technol. (Lebensmittel-Wissenschaft -Technol.)* 218, 117470. <https://doi.org/10.1016/j.lwt.2025.117470>.
- Li, Y., Leng, W., Xue, J., Yuan, L., Liu, H., Gao, R., 2023a. A multi-omics-based investigation into the flavor formation mechanisms during the fermentation of traditional Chinese shrimp paste. *Food Res. Int.* 166, 112585. <https://doi.org/10.1016/j.foodres.2023.112585>.
- Li, Y., Yuan, L., Liu, H., Liu, H., Zhou, Y., Li, M., Gao, R., 2023b. Analysis of the changes of volatile flavor compounds in a traditional Chinese shrimp paste during fermentation based on electronic nose, SPME-GC-MS and HS-GC-IMS. *Food Sci. Hum. Wellness* 12 (1), 173–182. <https://doi.org/10.1016/j.fshw.2022.07.035>.
- Liu, H., Wang, Z., Zhang, D., Shen, Q., Pan, T., Hui, T., Ma, J., 2019. Characterization of key aroma compounds in Beijing roasted duck by gas chromatography–olfactometry–mass spectrometry, odor-activity values, and aroma-recombination experiments. *J. Agric. Food Chem.* 67 (20), 5847–5856. <https://doi.org/10.1021/acs.jafc.9b01564>.
- Lu, K., Liu, L., Xu, Z., Xie, W., 2022. The analysis of volatile compounds through flavoromics and machine learning to identify the origin of traditional Chinese fermented shrimp paste from different regions. *LWT–Food Sci. Technol.* 171, 114096. <https://doi.org/10.1016/j.lwt.2022.114096>.
- Lv, X., Li, Y., Cui, T., Sun, M., Bai, F., Li, X., Li, J., Yi, S., 2020. Bacterial community succession and volatile compound changes during fermentation of shrimp paste from Chinese Jinzhou region. *LWT–Food Sci. Technol.* 122, 108998. <https://doi.org/10.1016/j.lwt.2019.108998>.
- Martínez-Cuesta, M.D.C., Peláez, C., Requena, T., 2013. Methionine metabolism: major pathways and enzymes involved and strategies for control and diversification of volatile sulfur compounds in cheese. *Crit. Rev. Food Sci. Nutr.* 53 (4), 366–385. <https://doi.org/10.1080/10408398.2010.536918>.
- Nierop Groot, Masja N., de Bont Jan, A.M., 1999. Involvement of manganese in conversion of phenylalanine to benzaldehyde by lactic acid bacteria. *Appl. Environ. Microbiol.* 65 (12), 5590–5593. <https://doi.org/10.1128/AEM.65.12.5590-5593.1999>.
- Park, S.-K., Jo, D.-M., Yu, D., Khan, F., Lee, Y.B., Kim, Y.-M., 2020. Reduction of trimethylamine off-odor by lactic acid bacteria isolated from Korean traditional fermented food and their in situ application. *J. Microbiol. Biotechnol.* 30 (10), 1510–1515. <https://doi.org/10.4014/jmb.2005.05007>.
- Shahidi, F., Abad, A., 2019. Lipid-derived flavours and off-flavours in food. In: Melton, L., Shahidi, F., Varelis, P. (Eds.), *Encyclopedia of Food Chemistry*. Academic Press, pp. 182–192. <https://doi.org/10.1016/B978-0-08-100596-5.21666-1>.
- Simons, T.J., McNeil, C.J., Pham, V.D., Suh, J.H., Wang, Y., Slupsky, C.M., Guinard, J.-X., 2019. Evaluation of California-grown blood and cara cara oranges through consumer testing, descriptive analysis, and targeted chemical profiling. *J. Food Sci.* 84 (11), 3246–3263. <https://doi.org/10.1111/1750-3841.14820>.
- Wang, S., Hu, M., Zhao, L., Liu, Q., Cao, R., 2022. Changes in lipid profiles and volatile compounds of shrimp (*Penaeus vannamei*) submitted to different cooking methods. *Int. J. Food Sci. Technol.* 57 (7), 4234–4244. <https://doi.org/10.1111/ijfs.15747>.

- Wang, S., Jian, C., Zhao, L., Sun, H., Liu, Q., Cao, R., 2025. Relationship between physicochemical properties, non-volatile substances, and microbial diversity during the processing of dry-cured Spanish mackerel. *Food Res. Int.* 200, 115501. <https://doi.org/10.1016/j.foodres.2024.115501>.
- Wu, S., Yang, J., Dong, H., Liu, Q., Li, X., Zeng, X., Bai, W., 2021. Key aroma compounds of Chinese dry-cured Spanish mackerel (*Scomberomorus niphonius*) and their potential metabolic mechanisms. *Food Chem.* 342, 128381. <https://doi.org/10.1016/j.foodchem.2020.128381>.
- Wang, X., Huang, M., Yao, Y., Yu, J., Cui, H., Hayat, K., Zhang, X., Ho, C.T., 2024. Difference comparison of characteristic aroma compounds between braised pork cooked by traditional open-fire and induction cooker and the potential formation cause under electromagnetic cooking. *Food Res. Int.* 188, 114506. <https://doi.org/10.1016/j.foodres.2024.114506>.
- Xiao, Y., Huang, Y., Chen, Y., Xiao, L., Zhang, X., Yang, C., Li, Z., Zhu, M., Liu, Z., Wang, Y., 2022. Discrimination and characterization of the volatile profiles of five Fu brick teas from different manufacturing regions by using HS-SPME/GC-MS and HS-GC-IMS. *Curr. Res. Food Sci.* 5, 1788–1807. <https://doi.org/10.1016/j.crf.2022.09.024>.
- Yang, X., Chen, Q., Liu, S., Hong, P., Zhou, C., Zhong, S., 2024. Characterization of the effect of different cooking methods on volatile compounds in fish cakes using a combination of GC-MS and GC-IMS. *Food Chem. X* 22, 101291. <https://doi.org/10.1016/j.fochx.2024.101291>.
- Yang, Z., Wu, R., Wei, X., Zhang, Z., Wang, W., Liu, A., Yang, J., Ji, C., Liang, H., Zhang, S., Lin, X., 2021. Moderate fermentation contributes to the formation of typical aroma and good organoleptic properties: a study based on different brands of Chouguiyu. *LWT-Food Sci. Technol.* 152, 112325. <https://doi.org/10.1016/j.lwt.2021.112325>.
- Yao, Y., Huang, M., Wang, X., Yu, J., Cui, H., Hayat, K., Zhang, X., Ho, C.-T., 2024. Characteristic volatile compounds contributed to aroma of braised pork and their precursor sources. *Food Chem.* 459, 140335. <https://doi.org/10.1016/j.foodchem.2024.140335>.
- Yu, J., Lu, K., Dong, X., Xie, W., 2022a. *Virgibacillus* sp. SK37 and *Staphylococcus nepalensis* JS11 as potential starters to improve taste of shrimp paste. *LWT-Food Sci. Technol.* 154, 112657. <https://doi.org/10.1016/j.lwt.2021.112657>.
- Yu, J., Lu, K., Zi, J., Yang, X., Xie, W., 2022b. Characterization of aroma profiles and aroma-active compounds in high-salt and low-salt shrimp paste by molecular sensory science. *Food Biosci.* 45, 101470. <https://doi.org/10.1016/j.fbio.2021.101470>.
- Zang, B., Li, S., Michel, F.C., Li, G., Zhang, D., Li, Y., 2017. Control of dimethyl sulfide and dimethyl disulfide odors during pig manure composting using nitrogen amendment. *Bioresour. Technol.* 224, 419–427. <https://doi.org/10.1016/j.biortech.2016.11.023>.
- Zhang, H., Huang, D., Pu, D., Zhang, Y., Chen, H., Sun, B., Ren, F., 2020. Multivariate relationships among sensory attributes and volatile components in commercial dry porcini mushrooms (*Boletus edulis*). *Food Res. Int.* 133, 109112. <https://doi.org/10.1016/j.foodres.2020.109112>.
- Zhang, L., Cao, Y., Tong, J., Xu, Y., 2019. An alkylpyrazine synthesis mechanism involving l-threonine-3-dehydrogenase describes the production of 2,5-dimethylpyrazine and 2,3,5-trimethylpyrazine by *Bacillus subtilis*. *Appl. Environ. Microbiol.* 85 (24), e01807. <https://doi.org/10.1128/AEM.01807-19>, 19.
- Zhao, Y., He, W., Zhan, P., Geng, J., Wang, P., Tian, H., 2024. A comprehensive analysis of aroma quality and perception mechanism in ginger-infused stewed beef using instrumental analysis, sensory evaluation and molecular docking. *Food Chem.* 460, 140435. <https://doi.org/10.1016/j.foodchem.2024.140435>.